Modulation of Proton-Coupled Electron Transfer through Molybdenum-quinonoid Interactions

Justin T. Henthorn and Theodor Agapie*
Division of Chemistry and Chemical Engineering, California Institute of Technology, Pasadena, CA 91125

I. Experimental Details

General considerations:

Unless indicated otherwise, reactions performed under inert atmosphere were carried out in oven-dried glassware in a glovebox under a nitrogen atmosphere purified by circulation through RCI-DRI 13X-0408 Molecular Seives 13X, 4x8 Mesh Beads and BASF PuriStar® Catalyst R3-11G, 5x3 mm (Research Catalysts, Inc.). Solvents for all reactions were purified by Grubbs' method.[1] CD_3CN and CD_2Cl_2 were purchased from Cambridge Isotope Laboratories and distilled from CaH_2 prior to use. Alumina and Celite were activated by heating under vacuum at 200 °C for 24 hours. ^1H, ^{19}F, and ^{31}P NMR spectra were recorded on Varian Mercury 300 MHz spectrometers at ambient temperature, unless denoted otherwise. ^{13}C NMR spectra were recorded on a Varian INOVA-500 MHz spectrometer. ^1H and ^{13}C NMR chemical shifts are reported with respect to internal solvent: 1.94 ppm and 118.26 for CD_3CN, and 5.32 ppm and 53.84 ppm for CD_2Cl_2, respectively. ^{19}F and ^{31}P NMR chemical shifts are reported with respect to an external standard of C_6F_6 (-164.9 ppm) and 85% H_3PO_4 (0.0 ppm).

Powder and thin film ATR-IR measurements were obtained by placing a powder or drop of solution of the complex on the surface of a Bruker APLHA ATR-IR spectrometer probe and allowing the solvent to evaporate (Platinum Sampling Module, diamond, OPUS software package) at 2 cm^{-1} resolution. Solution IR spectra were recorded on a Thermo-Fisher Scientific Nicolet 6700 FTIR spectrometer using a CaF_2 plate solution cell. Fast atom bombardment-mass spectrometry (FAB-MS) analysis was performed with a JEOL JMS-600H high-resolution mass spectrometer. Gas chromatography-mass spectrometry (GC-MS) analysis was performed upon filtering the sample through a plug of silica gel. Electrochemical measurements were recorded with a Pine Instrument Company AFCBP1 bipotentiostat using the AfterMath software package. Cyclic voltammograms and square-wave voltammograms were recorded on ca. 2 mM solutions of the relevant complex in the glovebox at 20 °C with an auxiliary Pt-coil electrode, a Ag/Ag^+ reference electrode (0.01 M $AgNO_3$, 0.1 M [^{n}Bu4N$^+$][PF_6^-] in MeCN), and a 3.0 mm glassy carbon electrode disc (BASI). The electrolyte solution was 0.1 M [^{n}Bu4N$^+$][PF_6^-] in MeCN. All reported values are referenced to an internal ferrocene/ferrocenium couple. Elemental analysis was conducted by Robertson Microlit Labs (Ledgewood, NJ).

Unless otherwise noted all chemical reagents were purchased from commercial sources and used without further purification. AgOTf, 2,3-dichloro-5,6-dicyano-1,4-benzoquinone and benzo-15-crown-5 were purchased from Sigma Aldrich and used as received. 2,6-di-*tert*-butyl-4-methylpyridine, 4-*tert*-butylphenol, 2-nitroaniline, and [2,2,2]-diazobicyclooctane were purchased from Sigma Aldrich and sublimed prior to use. $PhICl_2$,[2] BnK,[3] **1**,[4] **4**,[4] **8**[4], and Fetizon's reagent (Ag_2CO_3 on Celite)[5] were prepared using literature procedures. Assignments of NMR spectra are given corresponding to the following numbering scheme:

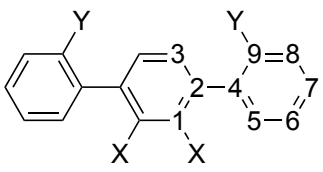

Synthesis of bis(benzo-15-crown-5)potassium [1,4-bis(2-(diisopropylphosphino)phenyl)-2,3-semicatecholate]tricarbonylmolybdenum(0) (9)

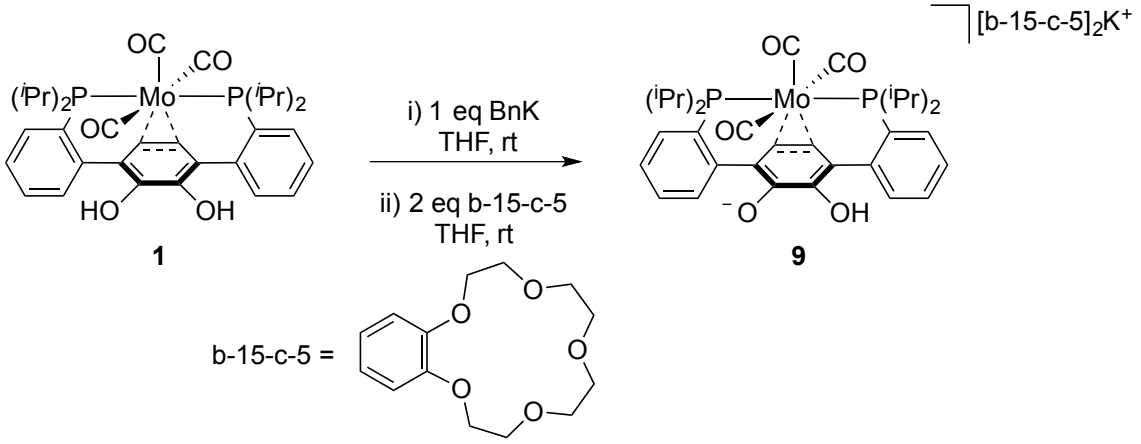

To a solution of **1** (0.0623 g, 0.0924 mmol) in THF (2 mL) was added dropwise a solution of BnK (0.0118 g, 0.0906 mmol) in THF (2 mL). Upon complete addition, a solution of benzo-15-crown-5 (0.0507 g, 0.189 mmol) in THF (2 mL) and the mixture was stirred at room temperature for 30 minutes. The volatiles were then removed under reduced pressure, and the resulting residue was triturated with Et_2O (5 mL) and the solid collected on a pad of celite. The solid was then dissolved in benzene (5 mL), filtered through celite, and concentrated in vacuo to afford the desired product as an orange powder (0.0756 g, 66%). ^{1}H NMR (300 MHz, CD_3CN , 25 °C), δ(ppm): 9.22 (s, br, 1 H, O–*H*), 8.04 (d, 8 Hz, 2 H, Ar-C*H*), 7.91 (d, 8 Hz, 2 H, Ar-C*H*), 7.38 (t, 8 Hz, 2 H, Ar-C*H*), 7.25 (t, 8 Hz, 2 H, Ar-C*H*), 6.91 (m, 2 H, crown Ar-C*H*), 6.81 (m, 2 H, crown Ar-C*H*), 5.38 (t, 4.9 Hz, 2 H, quinonoid Ar-C_3H), 3.91 (m, 4 H, crown O–CH_2), 3.66 (m, 8 H, crown O–CH_2), 3.66 (m, 8 H, crown O–CH_2), 3.57 (m, 4 H, crown O–CH_2), 2.93 (m, 2 H, PC*H*$(CH_3)_2$), 2.48 (m, 2 H, PC*H*$(CH_3)_2$), 1.42 (m, 6 H, PCH(C*H*$_3)_2$), 1.31 (m, 6 H, PCH(C*H*$_3)_2$), 0.96 (m, 6 H, PCH(C*H*$_3)_2$), 0.90 (m, 6 H, PCH(C*H*$_3)_2$). ^{31}P NMR (121 MHz, CD_3CN , 25 °C), δ(ppm): 51.42 (s). ^{13}C NMR (126 MHz, CD_3CN , 25 °C), δ(ppm): 229.15 (t, 10 Hz, Mo-*C*O), 216.66 (t, 10 Hz, Mo-*C*O), 211.78 (t, 10 Hz, Mo-*C*O), 149.80 (s, Ar-C_1), 148.65 (s, crown Ar-*C*–O), 133.03 (s, Ar-C*H*), 132.29 (s, Ar-C*H*), 131.73 (s, Ar-C*H*), 130.73 (s, Ar-C*H*), 128.59 (s, Ar-C*H*), 126.62 (s, Ar-C*H*), 124.95 (s, Ar-C*H*), 122.43 (s, crown Ar-*C*H), 120.19 (s, Ar-*C*), 114.32 (s, crown Ar-*C*H), 86.58 (s, C_3), 69.49 (s, crown O–CH_2), 68.75 (s, crown O–CH_2), 68.26 (s, crown O–CH_2), 67.91 (s, crown O–CH_2), 34.65 (t, P*C*H$(CH_3)_2$), 31.16 (t, P*C*H$(CH_3)_2$), 20.31 (t, PCH(*C*H$_3)_2$), 19.92 (t, PCH(*C*H$_3)_2$), 19.53 (s, PCH(*C*H$_3)_2$), 19.52 (s, PCH(*C*H$_3)_2$). IR (THF), ν_{CO} (cm^{-1}): 1875, 1605. Anal. Calcd for [**9**], $C_{61}H_{79}KMoO_{15}P_2$: C, 58.65; H, 6.37. Found: C, 57.33; H, 6.10.

Synthesis of bis(benzo-15-crown-5)potassium [1,4-bis(2-bromophenyl)-2,3-semicatecholate] (10)

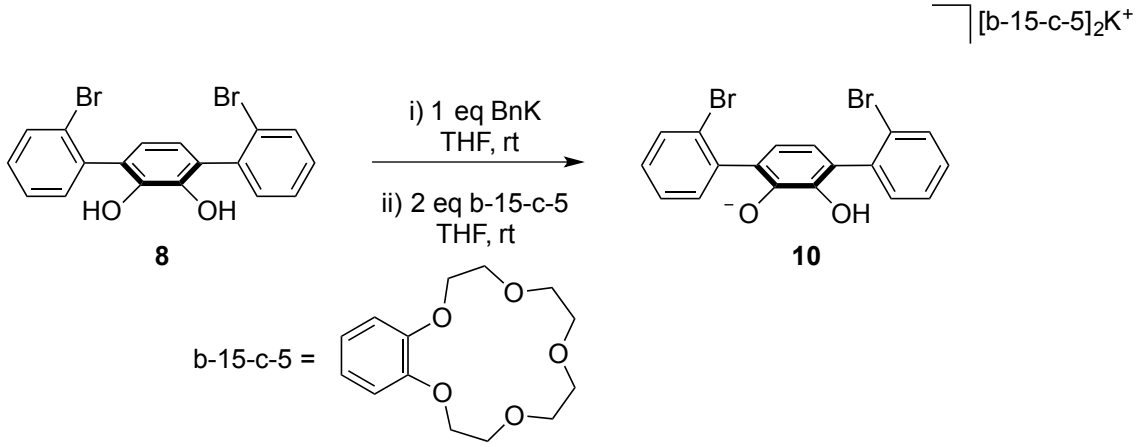

To a solution of **8** (0.0998 g, 0.238 mmol) in THF (2 mL) was added dropwise a solution of BnK (0.0309 g, 0.237 mmol) in THF (2 mL). Upon complete addition, a solution of benzo-15-crown-5 (0.1351 g, 0.504 mmol) in THF (2 mL) and the mixture was stirred at room temperature for 30 minutes. The volatiles were then removed under reduced pressure, and the resulting residue was triturated with Et_2O (5 mL) and the solid collected on a pad of celite. The solid was then dissolved in benzene (5 mL), filtered through celite, and concentrated in vacuo to afford the desired product as an orange powder (0.1213, 51%). ^{1}H NMR (300 MHz, CD_3CN , 25 °C), δ(ppm): 9.22 (s, br, 1 H, O–*H*), 8.04 (d, 8 Hz, 2 H, Ar-C*H*), 7.91 (d, 8 Hz, 2 H, Ar-C*H*), 7.38 (t, 8 Hz, 2 H, Ar-C*H*), 7.25 (t, 8 Hz, 2 H, Ar-C*H*), 6.91 (m, 2 H, crown Ar-C*H*), 6.81 (m, 2 H, crown Ar-C*H*), 5.38 (t, 4.9 Hz, 2 H, quinonoid Ar-C_3H), 3.91 (m, 4 H, crown O–CH_2), 3.66 (m, 8 H, crown O–CH_2), 3.66 (m, 8 H, crown O–CH_2), 3.57 (m, 4 H, crown O–CH_2), 2.93 (m, 2 H, PC*H*$(CH_3)_2$), 2.48 (m, 2 H, PC*H*$(CH_3)_2$), 1.42 (m, 6 H, PCH(C*H*$_3)_2$), 1.31 (m, 6 H, PCH(C*H*$_3)_2$), 0.96 (m, 6 H, PCH(C*H*$_3)_2$), 0.90 (m, 6 H, PCH(C*H*$_3)_2$). ^{31}P NMR (121 MHz, CD_3CN , 25 °C), δ(ppm): 51.42 (s). ^{13}C NMR (126 MHz, CD_3CN , 25 °C), δ(ppm): 228.21 (t, 10 Hz, Mo-*C*O), 215.71 (t, 10 Hz, Mo-*C*O), 210.83 (t, 10 Hz, Mo-*C*O), 148.86 (s, Ar-C_1), 147.70 (s, crown Ar-*C*–O), 132.09 (m), 131.35 (s, Ar-C*H*), 130.79 (s, Ar-C*H*), 129.78 (s, Ar-C*H*), 127.64 (s, Ar-C*H*), 125.68 (s, Ar-C*H*), 124.00 (s, Ar-C*H*), 121.48 (s, crown Ar-*C*H), 113.37 (s, crown Ar-*C*H), 85.63 (s, C_3), 68.55 (s, crown O–CH_2), 67.81 (s, crown O–CH_2), 67.32 (s, crown O–CH_2), 66.96 (s, crown O–CH_2), 33.70 (t, P*C*H$(CH_3)_2$), 30.22 (t, P*C*H$(CH_3)_2$), 19.37 (t, PCH(*C*H$_3)_2$), 18.98 (t, PCH(*C*H$_3)_2$), 18.58 (s, PCH(*C*H$_3)_2$), 18.57 (s, PCH(*C*H$_3)_2$). Anal. Calcd for [**3**], $C_{46}H_{51}Br_2KO_{12}$: C, 55.54; H, 5.17. Found: C, 54.15; H, 5.33.

Synthesis of 3,6-bis(2-bromophenyl)-1,2-benzoquinone (11)

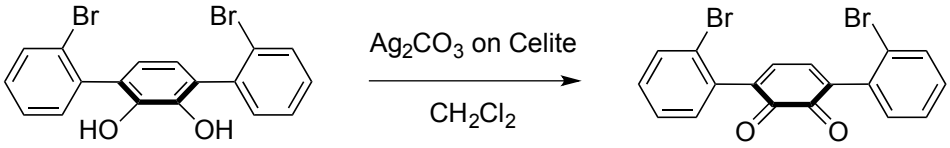

8 **11**

A round bottom flask was charged with **8** (200 mg, 0.476 mmol) dissolved in CH_2Cl_2 (40 mL). Silver carbonate on Celite (2.23 g, 3.90 mmol, 1.75 mmol Ag_2CO_3/g) was added with stirring. The reaction was allowed to stir for 30 minutes at room temperature. The reaction was then filtered over a pad of Celite and the filtrate concentrated *in vacuo* to yield a red-orange solid (198 mg, 99%). ^{1}H NMR (300 MHz, $CDCl_3$, 25 °C), δ(ppm): 7.72 – 7.61 (m, 2 H, Ar-C*H*), 7.43 – 7.24 (m, 6 H, Ar-C*H*), 7.13 (s, 2 H, Ar-C_3*H*). ^{13}C NMR (126 MHz, CD_3CN , 25 °C), δ(ppm): 178.27 (s, Ar-*C*=O), 142.26 (s, Ar-*C*), 137.96 (s, Ar-C_3H), 134.87 (s, Ar-*C*), 133.10 (s, Ar-*C*H), 131.02 (s, Ar-*C*H), 130.50 (s, Ar-*C*H), 127.41 (s, Ar-*C*H), 123.15 (s, Ar-*C*). MS (m/z): calcd, 417.9027 $[M]^+$; found, 417.9023 (FAB^+, $[M]^+$).

General procedure for determining the p*K*$_a$ of compounds 1, 2, 3 and 8

The pK_a values for compounds **1**, **2**, **3**, and **8** were determined via ^{1}H NMR spectroscopy and are the average of triplicate self-consistent trials, as has been described previously. The compound of interest was combined with an acid or base of known pK_a and the equilibrium populations were determined via ^{1}H NMR spectroscopy. All compounds exhibit rapid proton exchange on the NMR time-scale, such that the chemical shift can be used to determine the mole fraction of the species in solution via the equation $\chi_A = (\delta_{eq} - \delta_A)/(\delta_A - \delta_B)$, where χ_A is mole fraction of the acid, δ_e is the equilibrium chemical shift and δ_A and δ_B are the chemical shifts of the pure acid and the pure conjugate base, respectively. The value of χ_A was determined using well-resolved ^{1}H NMR signals, with good agreement observed between the independent calculations. The value used to determine the equilibrium concentration was the average of the independent caluclations. Once the equilibrium concentrations were determined, the equilibrium constant between the compound of interest and the acid/base of known pK_a was determined, and by using Hess's law the pK_a of the Mo complex (or **8**) was determined. The following acids/bases were used to determine the unknown pK_a's: 4-*tert*-butylphenol (pK_a = 27.45) for compound **1** and **8**; [2,2,2]-diazobicyclooctane (pK_a = 18.60) for compound **3**; 2-nitroaniline (pK_a = 4.80) for compound **2**. Representative ^{1}H NMR spectra of equilibrium mixtures used to calculate pKa's are given in Figure **S27**.

Reactions of 1, 2 and 8 with TEMPO and 11 with TEMPOH

1 and TEMPO: Compound **1** (0.0295 g, 0.0437 mmol) and TEMPO (0.0147 g, 0.0941 mmol) were combined in CD_3CN (0.6 mL) in a 1 dram vial and thoroughly mixed for 30 seconds until all of **1** had solubilized and the color had darkened from pale orange to red-orange. The solution was then transferred to an NMR tube and the ^{1}H and ^{31}P NMR spectra were recorded (Figure **S23**).

2 and TEMPO: Compound **2** (0.0225 g, 0.0238 mmol) and TEMPO (0.0082 g, 0.0525 mmol) were combined in CD_3CN (0.6 mL) in a 1 dram vial and thoroughly mixed for 30 seconds until all of **2** had solubilized and the color had darkened from pale orange to red-orange. The solution was then transferred to an NMR tube and the ^{1}H and ^{31}P NMR spectra were recorded (Figure **S24**).

8 and TEMPO: Compound **8** (0.0412 g, 0.0981 mmol) and TEMPO (0.0299 g, 0.191 mmol) were combined in CD_3CN (0.6 mL) in a 1 dram vial and thoroughly mixed for 30 seconds until all of **8** had solubilized. No color change was observed. The solution was then transferred to an NMR tube and the ^{1}H and ^{31}P NMR spectra were recorded (Figure **S25**).

11 and TEMPOH: Compound **11** (0.0100 g, 0.0239 mmol) and TEMPOH (0.0075 g, 0.0477 mmol) were combined in CD_3CN (0.6 mL) in a 1 dram vial and thoroughly mixed for 30 seconds until all of **11** had solubilized. The solution was then transferred to an NMR tube and the ^{1}H and ^{31}P NMR spectra were recorded, showing generation of compound **8** (Figure **S26**). The solution turned from a red orange to a pale pink within minutes.

II. Nuclear Magnetic Resonance Spectra

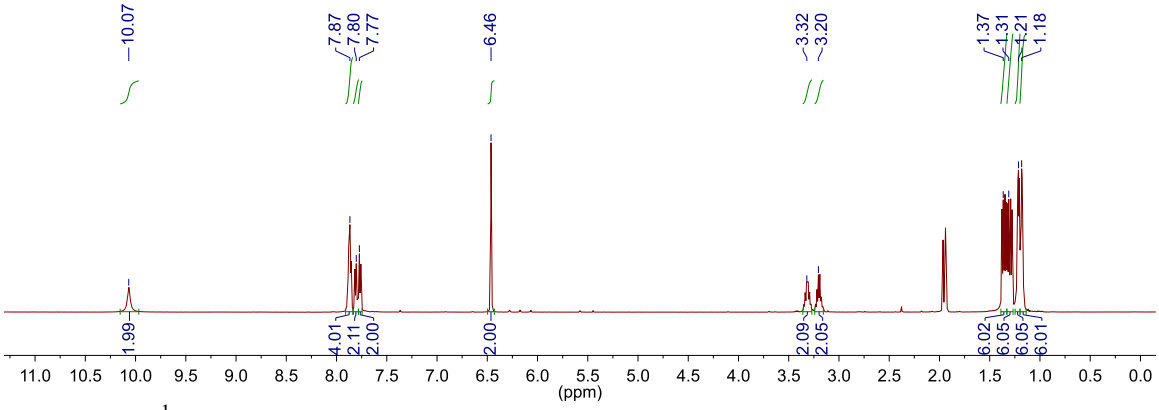

Figure S1. ^{1}H NMR spectrum of **2** in CD_3CN at 25 °C.

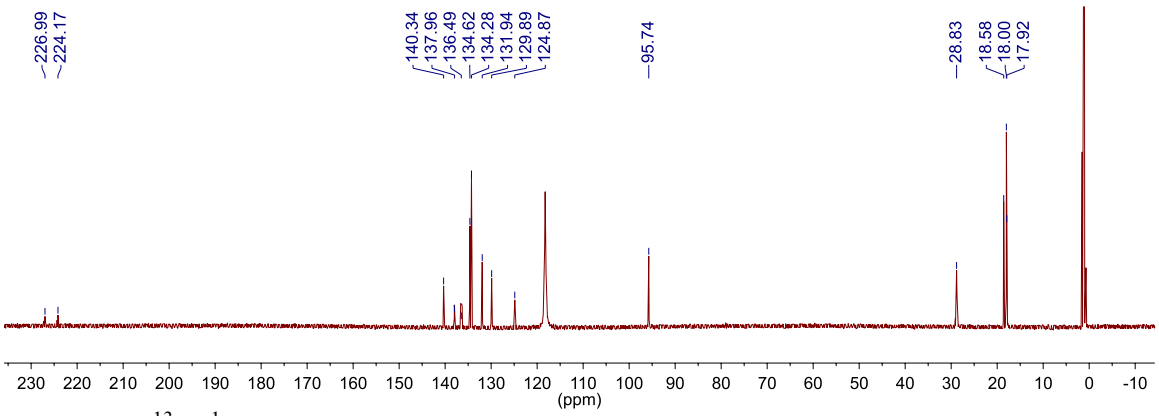

Figure S2. $^{13}C\{^{1}H\}$ NMR spectrum of **2** in CD_3CN at 25 °C.

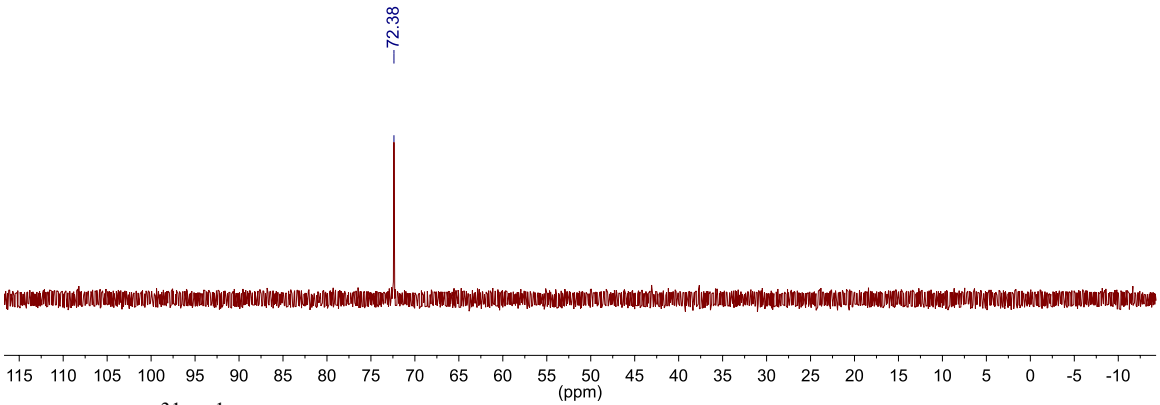

Figure S3. $^{31}P\{^{1}H\}$ NMR spectrum of **2** in CD_3CN at 25 °C.

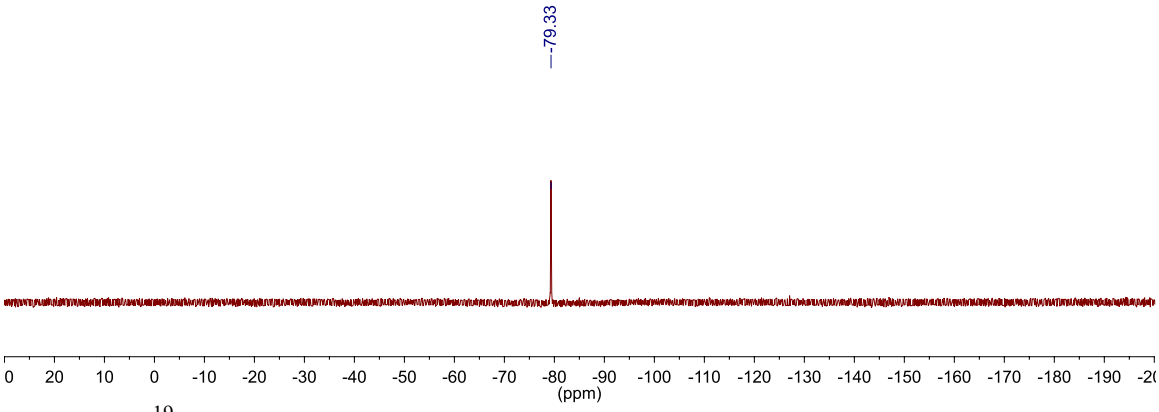

Figure S4. ^{19}F NMR spectrum of **2** in CD_3CN at 25 °C.

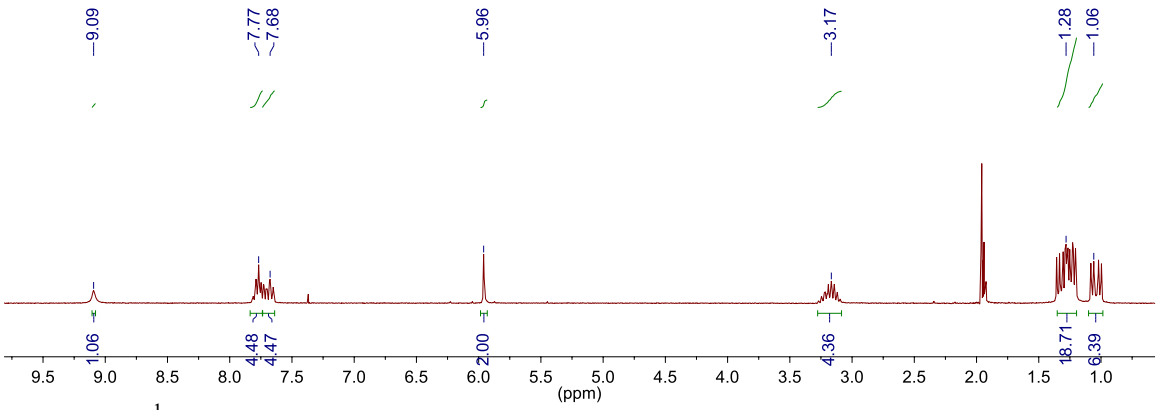

Figure S5. ^{1}H NMR spectrum of **3** in CD_3CN at 25 °C.

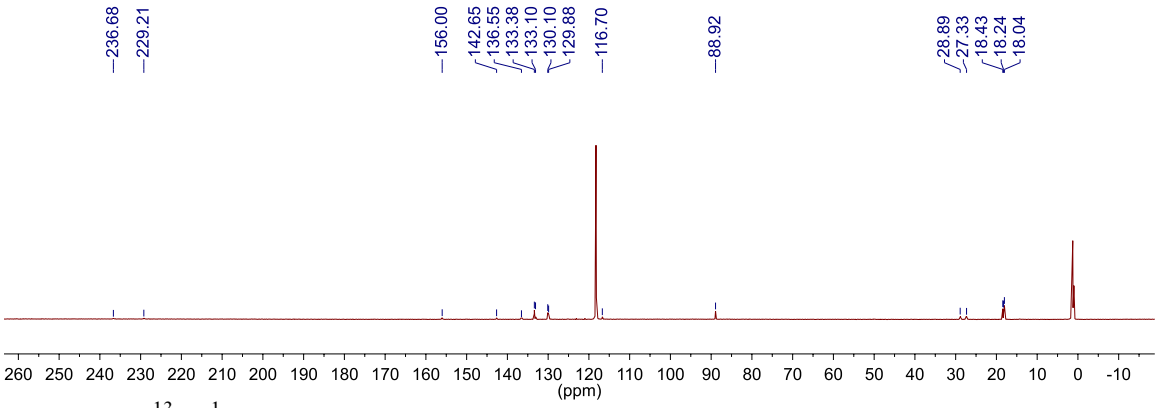

Figure S6. $^{13}C\{^{1}H\}$ NMR spectrum of **3** in CD_3CN at 25 °C.

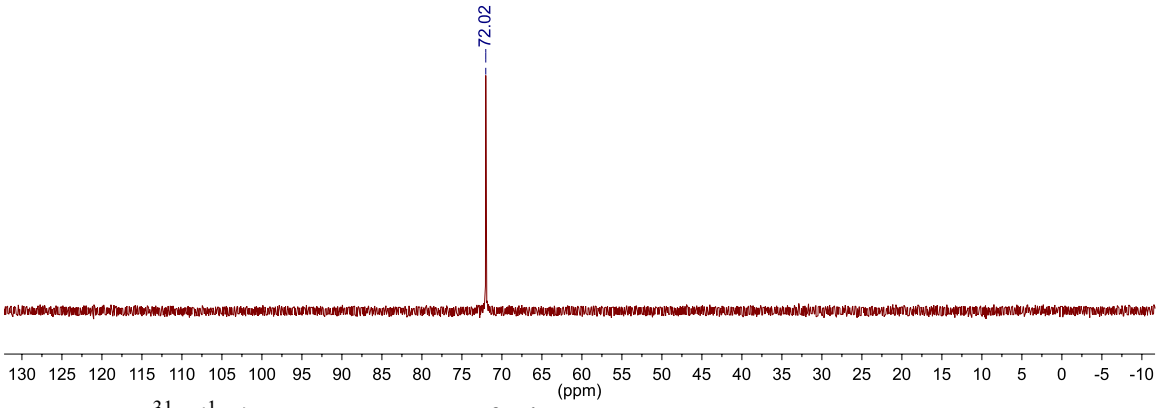

Figure S7. $^{31}P\{^{1}H\}$ NMR spectrum of **3** in CD_3CN at 25 °C.

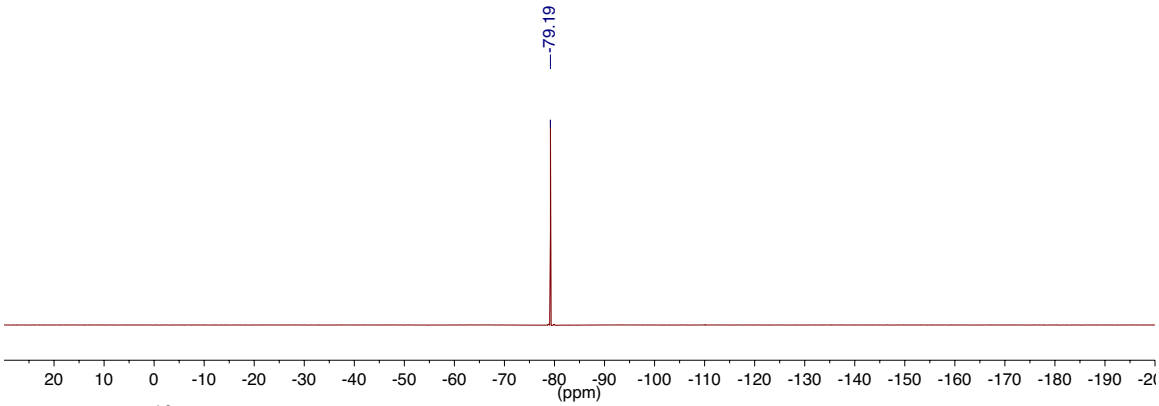

Figure S8. ^{19}F NMR spectrum of **3** in CD_3CN at 25 °C.

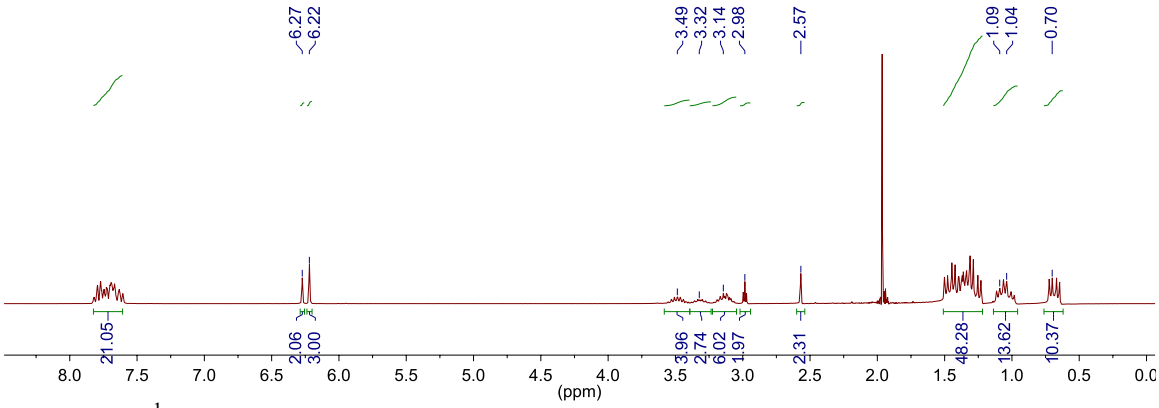

Figure S9. ^{1}H NMR spectrum of mixture of **5a** and **5b** in CD_3CN at 25 °C.

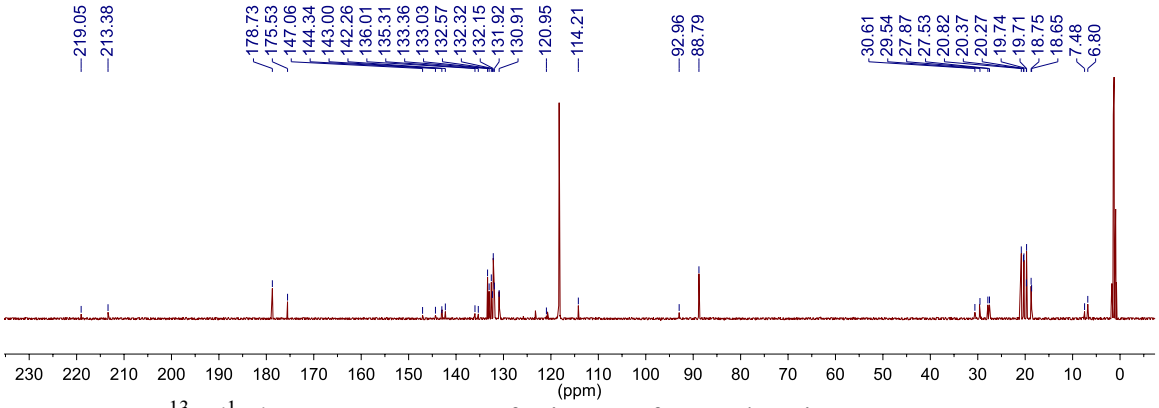

Figure S10. $^{13}C\{^{1}H\}$ NMR spectrum of mixture of **5a** and **5b** in CD_3CN at 25 °C.

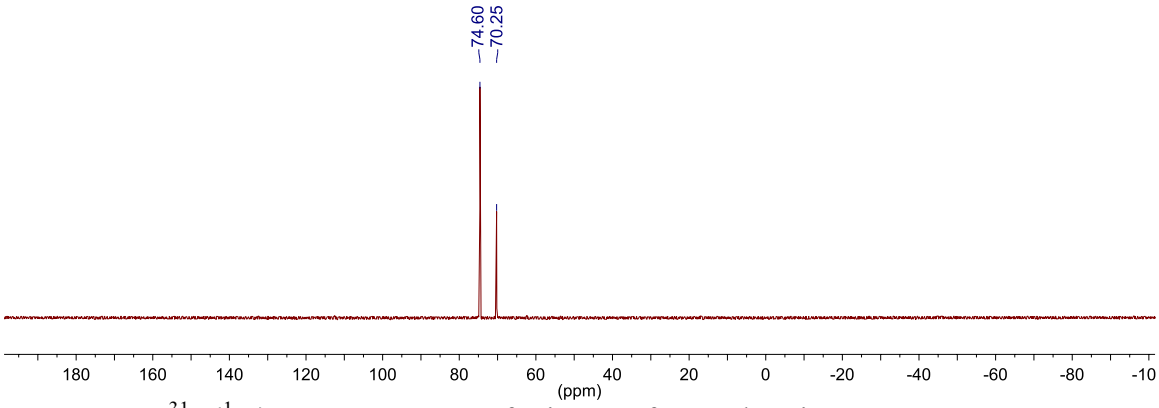

Figure S11. $^{31}P\{^{1}H\}$ NMR spectrum of mixture of **5a** and **5b** in CD_3CN at 25 °C.

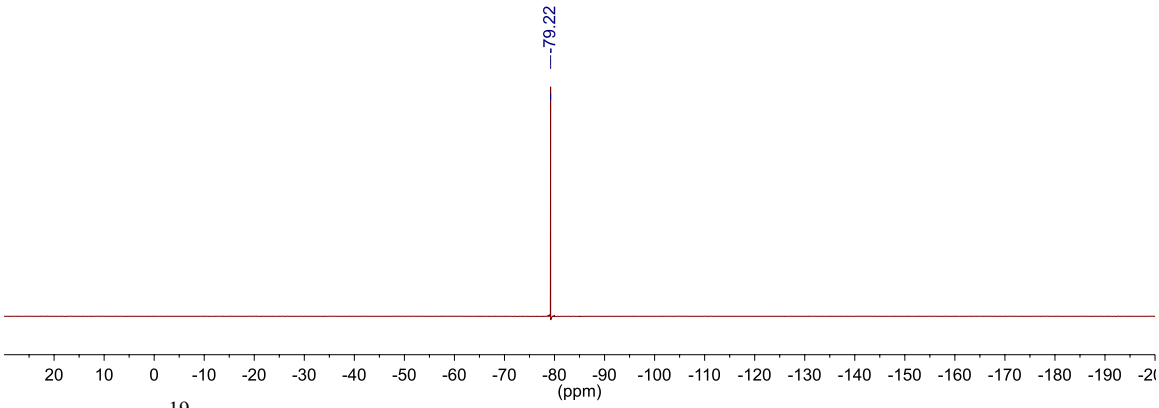

Figure S12. ^{19}F NMR spectrum of mixture of **5a** and **5b** in CD_3CN at 25 °C.

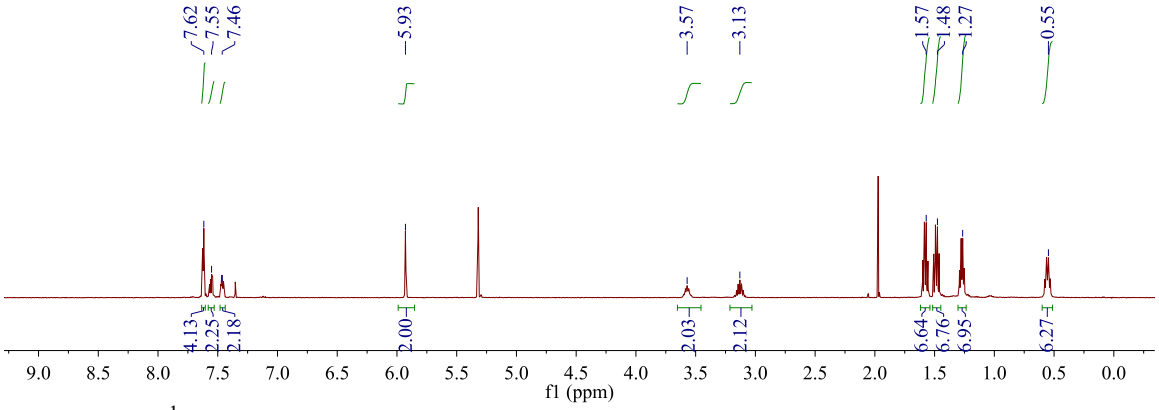

Figure S13. ^{1}H NMR spectrum of **6** in CD_2Cl_2 at 25 °C.

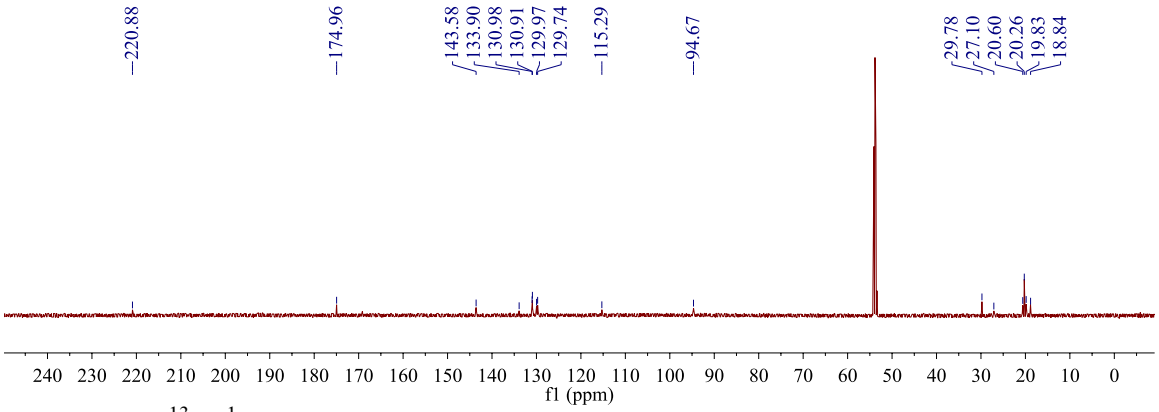

Figure S14. $^{13}C\{^{1}H\}$ NMR spectrum of **6** in CD_2Cl_2 at 25 °C.

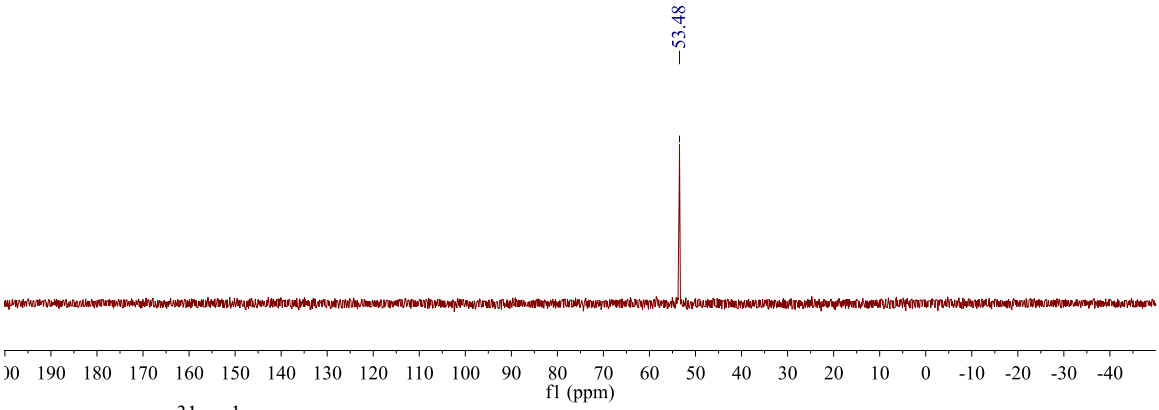

Figure S15. $^{31}P\{^{1}H\}$ NMR spectrum of **6** in CD_2Cl_2 at 25 °C.

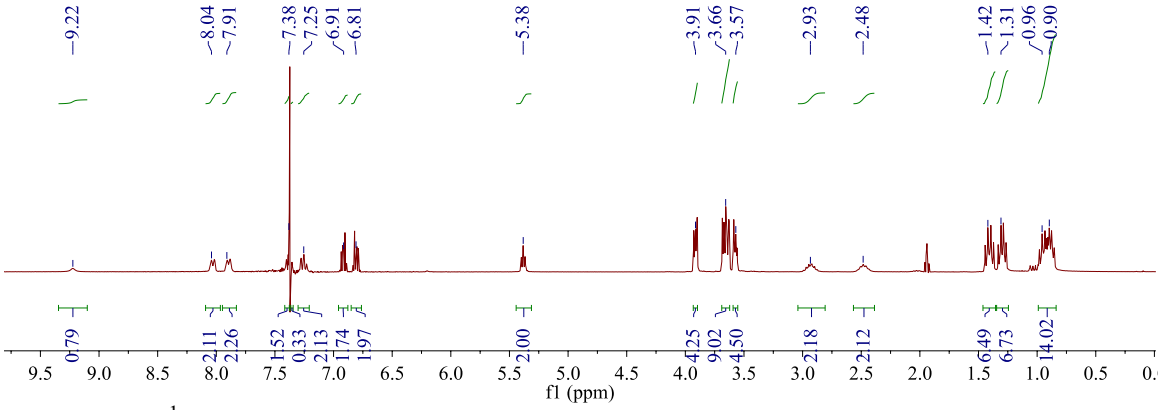

Figure S16. ^{1}H NMR spectrum of **9** in CD_3CN at 25 °C.

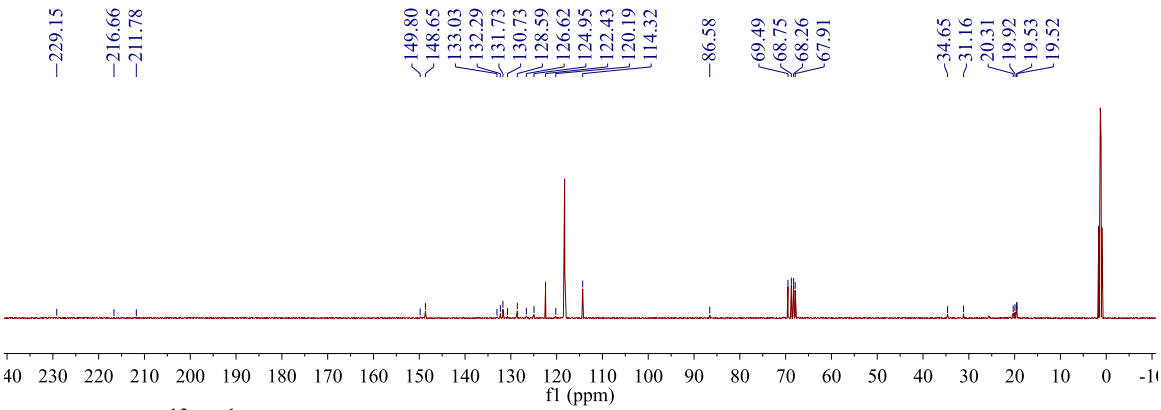

Figure S17. $^{13}C\{^{1}H\}$ NMR spectrum of **9** in CD_3CN at 25 °C.

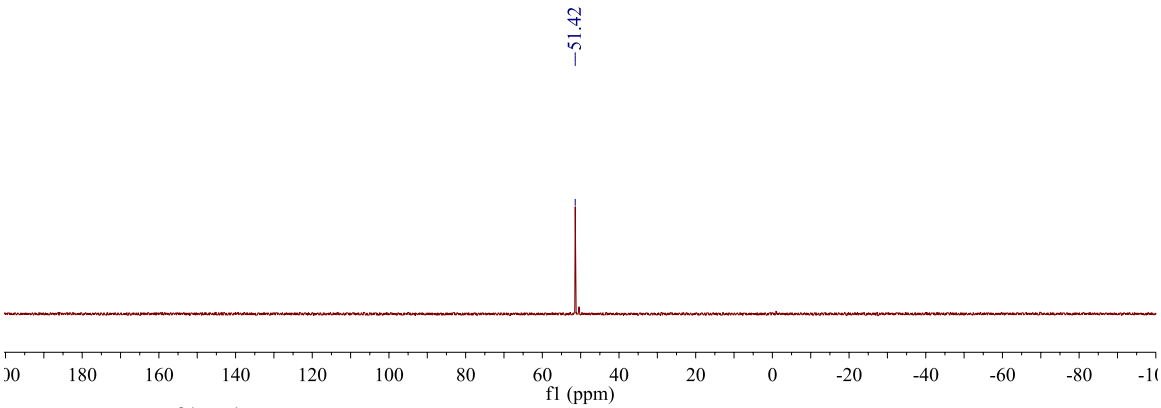

Figure S18. $^{31}P\{^{1}H\}$ NMR spectrum of **9** in CD_3CN at 25 °C.

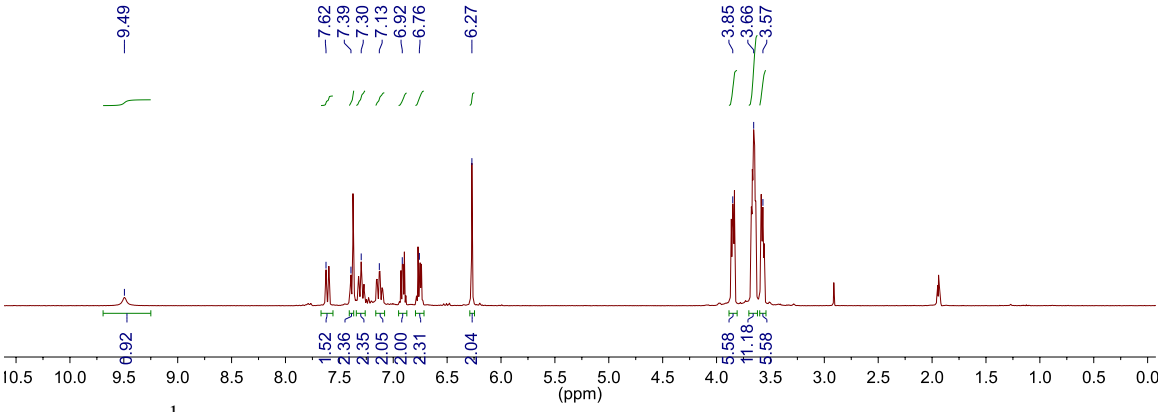

Figure S19. ^{1}H NMR spectrum of **10** in CD_3CN at 25 °C.

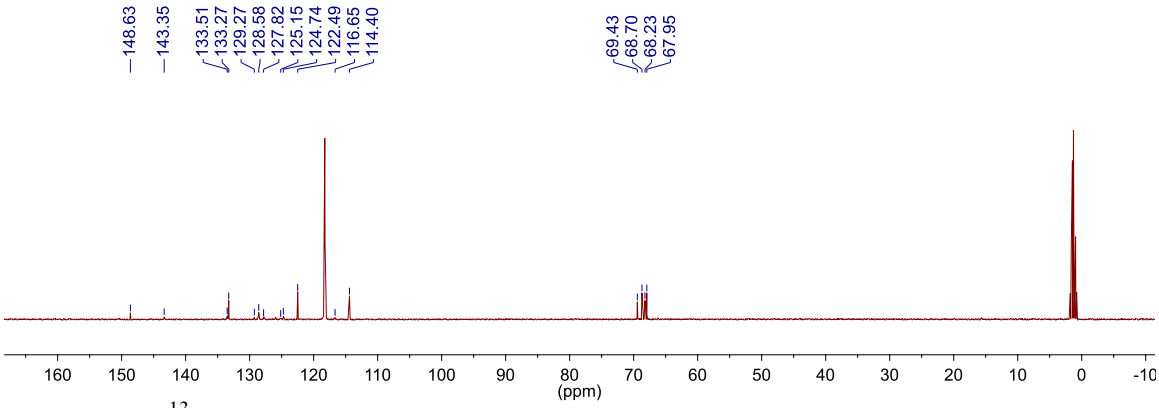

Figure S20. ^{13}C NMR spectrum of **10** in CD_3CN at 25 °C.

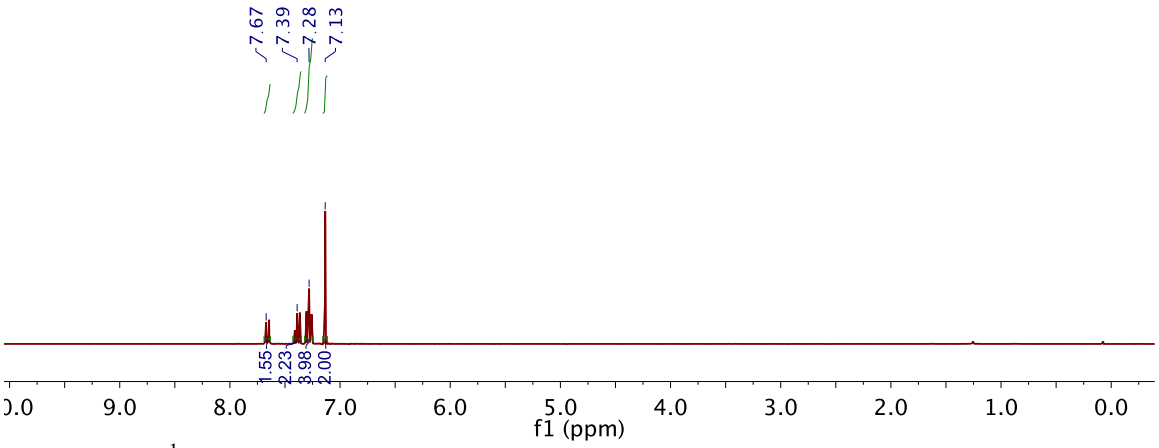

Figure S21. ^{1}H NMR spectrum of **11** in $CDCl_3$ at 25 °C.

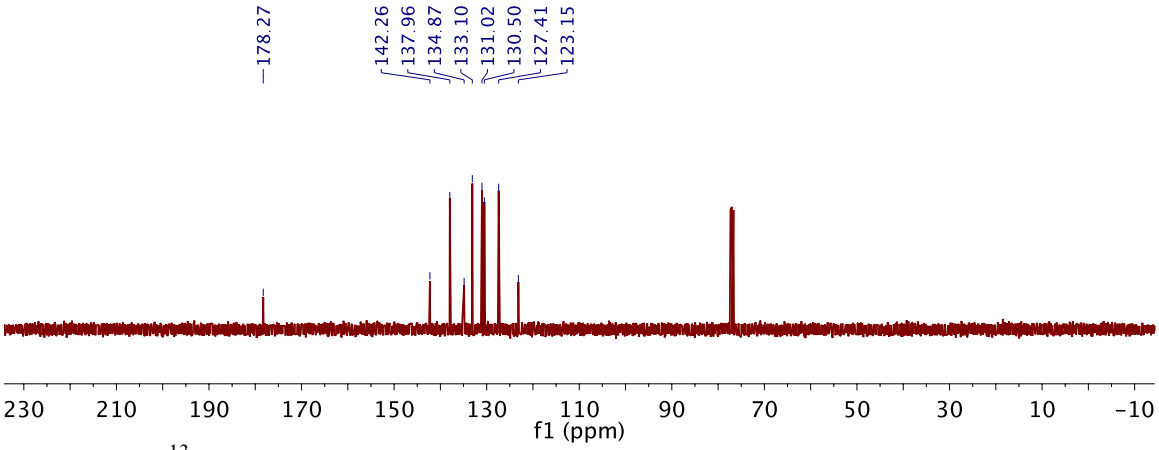

Figure S22. ^{13}C NMR spectrum of **11** in $CDCl_3$ at 25 °C.

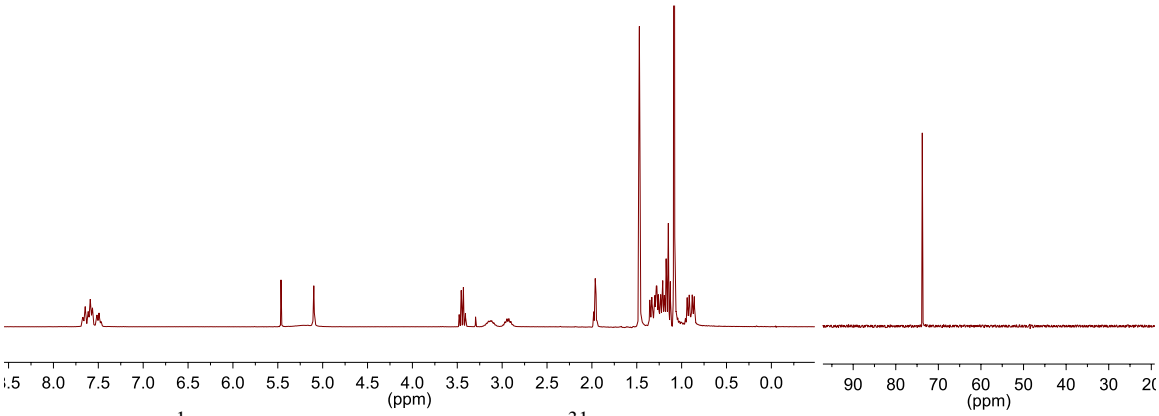

Figure S23. ^{1}H NMR spectrum (left) and ^{31}P NMR spectrum (right) of **1** and 2 equiv. TEMPO in CD_3CN at 25 °C after 10 min.

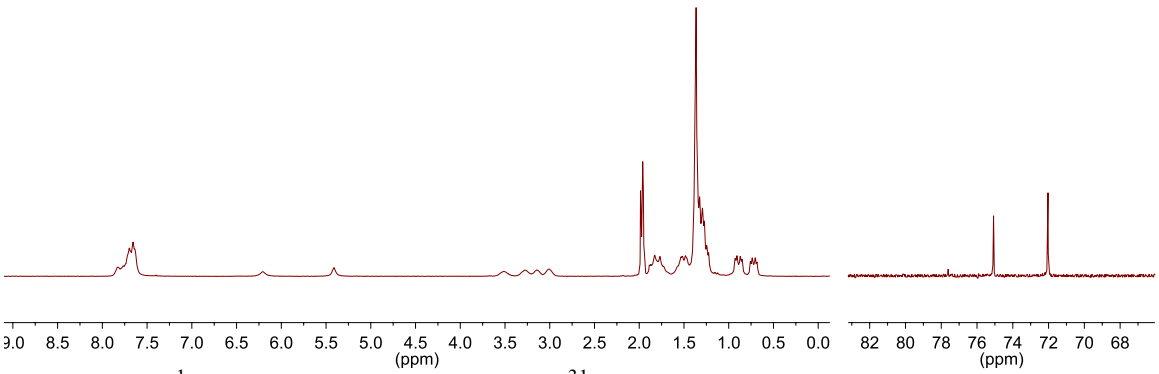

Figure S24. ^{1}H NMR spectrum (left) and ^{31}P NMR spectrum (right) of **2** and 2 equiv. TEMPO in CD_3CN at 25 °C after 10 min.

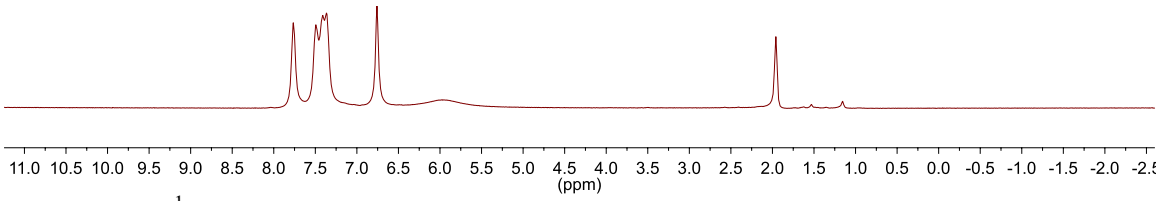

Figure S25. ^{1}H NMR spectrum of **8** and 2 equiv. TEMPO in CD_3CN at 25 °C after 10 min.

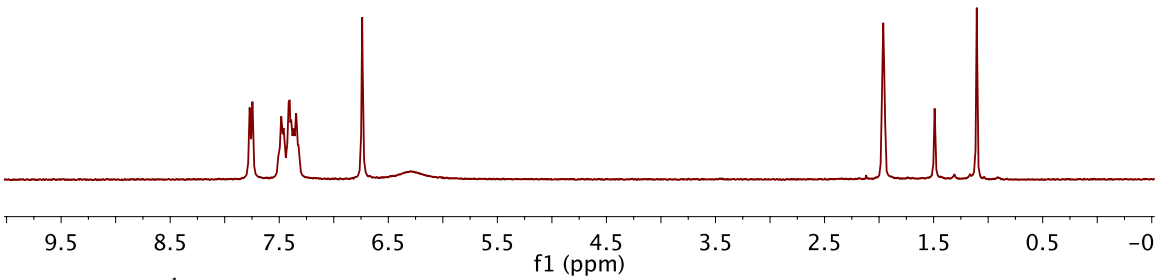

Figure S26. ^{1}H NMR spectrum of **11** and 2 equiv. TEMPOH in CD_3CN at 25 °C after 10 min.

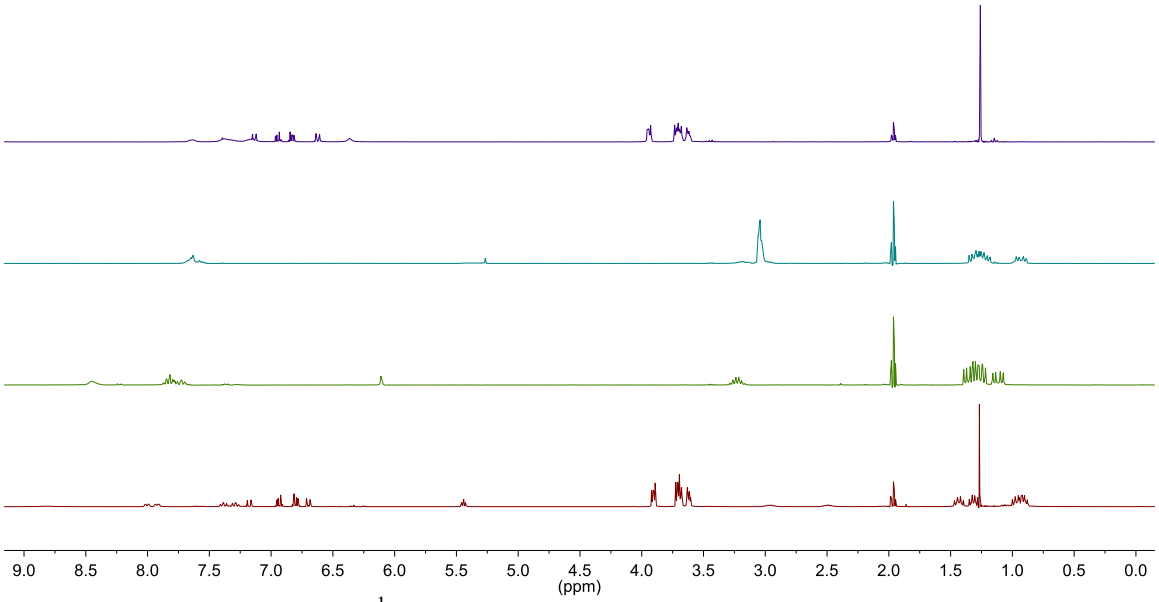

Figure S27. Representative ^{1}H NMR spectrum of equilibrium mixtures in CD_3CN of **9** and 4-^{t}BuPhOH (brown), **2** and 2-NO_2PhNH_2 (green), **3** and DABCO (teal), and **10** and 4-^{t}BuPhOH (purple) all recorded at 25 °C.

III. Estimation of O-H BDFE

Table S1. Thermochemical data for selected quinonoid compounds. Note that **1**, **2**, and **3** show irreversible redox events by cyclic voltammetry.

	$pK_{a(O–H)}$[a]	$E°_{Irr(O^-/O\cdot)}$[b]	Estimated $BDFE_{O–H}$[c]
1	25.89(9)	-0.770 V	73 kcal/mol
2	4.74(9)	0.220 V	67 kcal/mol
3	17.1(4)	-0.470 V	68 kcal/mol
8	26.3(1)	-0.630 V[d]	76 kcal/mol

[a]pK_a for first O–H determined via solution equilibria (see SI). [b]Irreversible oxidation potential for conjugate base determined via square-wave voltammetry. [c]Calculated using equation (1). [d]Reversible oxidation event.

IV. Crystallographic Information

CCDC 1469761-1469764 contain the supplementary crystallographic data for this paper. These data can be obtained free of charge from The Cambridge Crystallographic Data Centre via www.ccdc.cam.ac.uk/data_request/cif.

Refinement Details

In each case, crystals were mounted on a glass fiber or nylon loop using Paratone oil, then placed on the diffractometer under a nitrogen stream. Low temperature (100 K) X-ray data were obtained on a Bruker APEXII CCD based diffractometer (Mo sealed X-ray tube, K_α = 0.71073 Å) or a Bruker PHOTON100 CMOS based diffractometer (Mo micro-focus sealed X-ray tube, K_α = 0.71073 Å). All diffractometer manipulations, including data collection, integration, and scaling were carried out using the Bruker APEXII software.[6] Absorption corrections were applied using SADABS.[7] Space groups were determined on the basis of systematic absences and intensity statistics and the structures were solved by direct methods using XS[8], by intrinsic phasing using XT (incorporated into SHELXTL), or by charge flipping using Olex2[9] and refined by full-matrix least squares on F^2. All non-hydrogen atoms were refined using anisotropic displacement parameters. Hydrogen atoms were placed in the idealized positions and refined using a riding model. The structures were refined (weighed least squares refinement on F^2) to convergence. Graphical representation of structures with 50% probability thermal ellipsoids was generated using Diamond visualization software.[10]

Table S2. Crystal and refinement data for **3**, **5a•2NCMe**, **5b**, and **6**.

Compound	**3**	**5a•2NCMe**	**5b**	**6**
CCDC	1469761	1469762	1469763	1469764
empirical formula	$C_{33}H_{39}F_3MoO_7P_2S$	$C_{39}H_{50}F_{12}MoN_4O_3P_2Sb_2$	$C_{37}H_{44}F_6MoN_2O_9P_2S_2$	$C_{31}H_{38}Cl_2MoO_3P_2$
formula wt	794.61 g/mol	1252.23 g/mol	996.74 g/mol	687.39 g/mol
T (K)	100	100	100	100
a, Å	30.285(3)	10.005(1)	11.3464(4)	16.255(1)
b, Å	26.445(2)	27.668(2)	21.2519(8)	16.255(1)
c, Å	17.945(1)	19.306(1)	17.4117(7)	22.205(2)
α, deg	90	90	90	90
β, deg	93.729(2)	94.925(3)	94.171(1)	90
γ, deg	90	90	90	90
V, Å^3	14341(2)	5324.3(5)	4187.4(3)	5866.9(5)
Z	4	4	4	8
cryst syst	Monoclinic	Monoclinic	Monoclinic	Orthorhombic
space group	$P2_1/c$	$P2_1/n$	$P2_1/n$	Pbca
d_{calc}, g/cm^3	1.407	1.562	1.581	1.556
θ range, deg	2.18-33.14	1.29-38.57	2.629-43.71	1.83-45.29
μ , mm^{-1}	0.573	1.377	0.571	0.771
abs cor	Semi-empirical	Semi-empirical	Semi-empirical	Semi-empirical
GOF	1.070	1.132	1.058	0.954
R_1[a], wR_2[b] (I > 2sig(I))	0.0556, 0.1313	0.0409, 0.1502	0.0317, 0.0756	0.0338, 0.0868
Diffractometer	APEXII	APEXII	PHOTON100	APEXII

[a] $R_1 = \Sigma||F_o| - |F_c||/\Sigma|F_o|$. [b] $wR_2 = [\Sigma[w(F_o^2 - F_c^2)^2]/ \Sigma[w(F_o^2)^2]]^{1/2}$

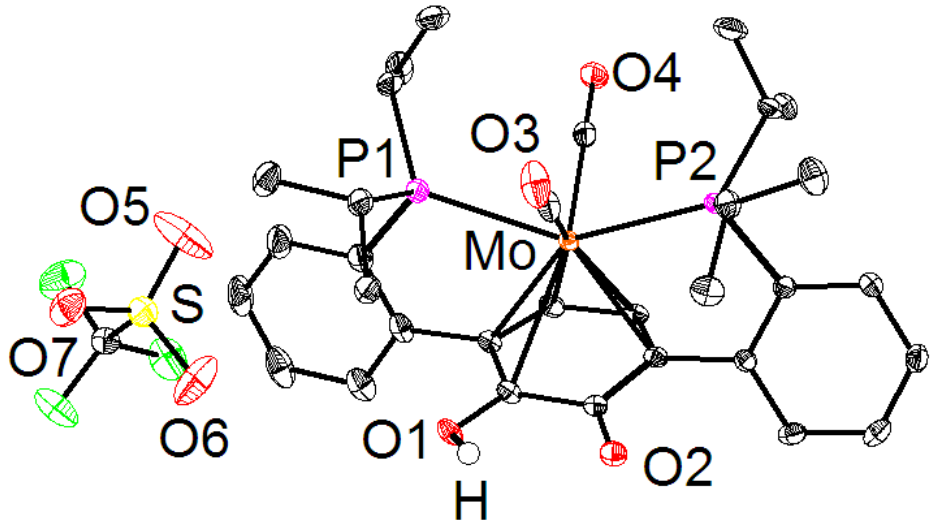

Figure S28. Structural drawing of **3** with 50% probability ellipsoids. Hydrogen atoms, and additional three Mo complexes and three triflate anions of the asymmetric unit are omitted for clarity. Carbon and fluorine atoms are shown in black and green, respectively.

Special Refinement Details for 3: One of the four triflate anions was positionally disordered and satisfactorily modeled as approximately a 50:50 mixture using "PART", "SAME", and "EADP" cards in SHELX. Two isopropyl groups were also positionally disordered and satisfactorily modeled as approximately 70:30 mixtures using "PART" cards in SHELX. Two DMF solvent molecules were highly disordered and could not be adequately modeled even with constraints. The electron density of these molecules was removed using the "solvent mask" function in Olex2.

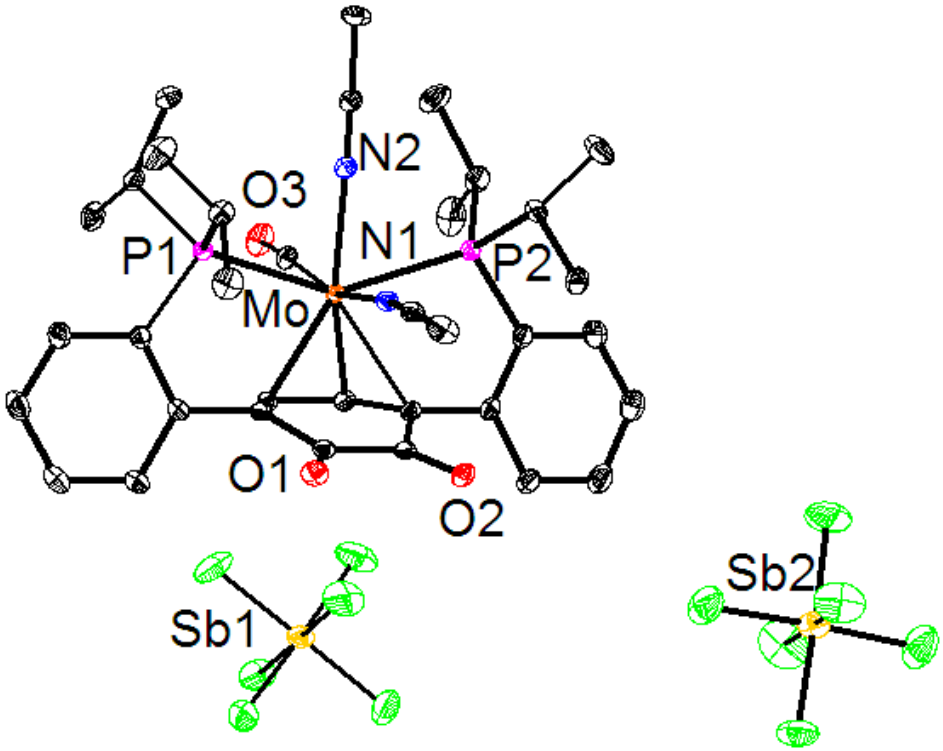

Figure S29. Structural drawing of **5a•2NCMe** with 50% probability ellipsoids. Hydrogen atoms and solvent molecules are omitted for clarity. Carbon and fluorine atoms are shown in black and green, respectively.

Special Refinement Details for 5a: Two acetonitrile solvent molecules were highly disordered and could not be adequately modeled even with constraints. The electron density of these molecules was removed using the "solvent mask" function in Olex2.

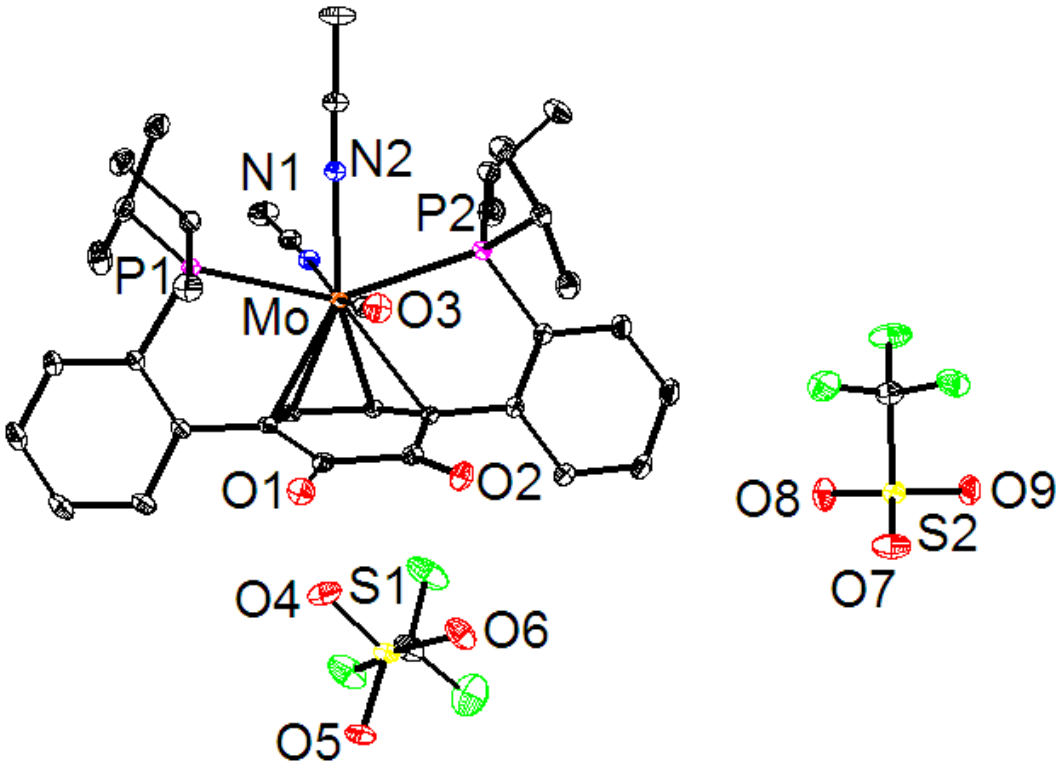

Figure S30. Structural drawing of **5b** with 50% probability ellipsoids. Hydrogen atoms are omitted for clarity. Carbon and fluorine atoms are shown in black and green, respectively.

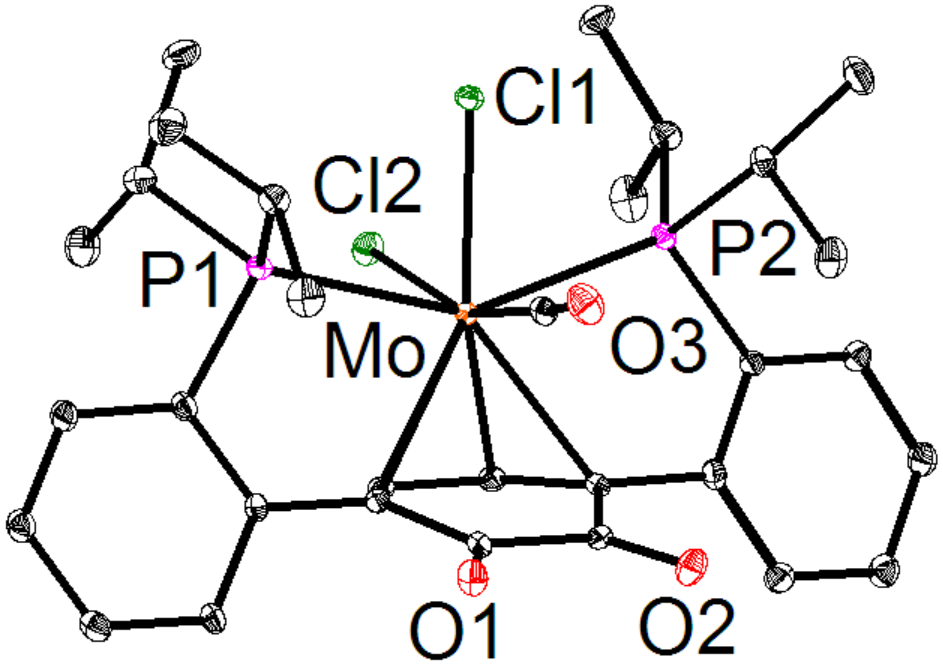

Figure S31. Structural drawing of **6** with 50% probability ellipsoids. Hydrogen atoms are omitted for clarity. Carbon atoms are shown in black.

V. References

(1) Pangborn, A.B.; Giardell, M.A.; Grubbs, R.H.; Rosen, R.K.; Timmers, F.J. *Organometallics* **1996**, *15*, 1518.
(2) Podgorsek, A.; Iskra, J. *Molecules* **2010**, *15*, 2857–2871.
(3) Schlosser, M.; Hartman, R. *Angew. Chem., Int. Ed.* **1973**, *12*, 508−509.
(4) Henthorn, J.T.; Lin, S.; Agapie, T. *J. Am. Chem. Soc.* 2015, 137 (4), pp 1458–1464.
(5) Balogh, V.; Fetizon, M.; Golfier, M. *J. Org. Chem.*, **1971**, *36* (10), pp 1339–1341
(6) APEX2, Version 2 User Manual, M86-E01078, Bruker Analytical X-ray Systems, Madison, WI, June 2006.
(7) Sheldrick, G.M. "SADABS (version 2008/1): Program for Absorption Correction for Data from Area Detector Frames", University of Göttingen, 2008.
(8) Sheldrick, G.M. (2008). Acta Cryst. A64, 112-122.
(9) Dolomanov, O.V. (2009). OLEX2. J. Appl. Cryst. **42**, 339-341.
(10) Brandenburg, K. (1999). DIAMOND. Crystal Impact GbR, Bonn, Germany.